Science & Technology Development Journal, 24(3):2031-2043

Open Access Full Text Article

Research Article

Effects of pressure angle on uneven wear of a tooth profile of an elliptical gear generated by ellipse involute

Nguyen Hong Thai, Phung Van Thom, Dang Bao Lam*

ABSTRACT

This paper presents a method to establish a mathematical model of an elliptical gears pair's tooth profile slip curve. The gear has an ellipse involute tooth profile generated by a rack cutter. The profile equation was developed based on the gearing theory with centrodes and center distance and consideration to conditions for avoiding undercutting. An elliptical involute curve and design parameters of the rack cutter were established corresponding to different points on the centrode of the elliptical gear. The profile equation was developed based on the theory of gearing with given centrodes and axis distance and consideration to conditions for avoiding undercutting. An elliptical involute curve and design parameters of the rack cutter determined corresponding to different points on the centrode of the elliptical gear. Wrote a number calculation program was in Matlab to examine and select appropriate pressure angles to limit the slippage between the mating teeth, to reduce wearing and enhance the lifespan of the elliptical gear pair. Case studies were also presented to confirm the influence of the pressure angle on the profile slippage phenomenon and select the rack cutter's pressure angle to reduce uneven wearing between the teeth of one elliptical gear. The survey results show that when the pressure angle of the rack cutter is large, the profile wear will occur faster since the ramp tooth rib, shorter length of the line of action, and pointed tooth tip. These research results are meaningful in selecting the rack cutter's pressure angle to gear the non-circular gear has tooth profile is an involute ellipse curve.

Key words: elliptical gear, ellipse involute, rack cutter, pressure angle, specific sliding

School of mechanical engineering, Hanoi University of Science and Technology

Correspondence

Dang Bao Lam, School of mechanical engineering, Hanoi University of Science and Technology

Email: lam.dangbao@hust.edu.vn

History

- Received: 2021-03-21
- Accepted: 2021-07-25
- Published: 2021-08-11

DOI : 10.32508/stdj.v24i3.2537

INTRODUCTION

Elliptical gears have been studied and applied more and more in various fields such as agricultural machines, measurement equipment, medical instruments, etc. Recently, Guo [1] implemented oval gears to design the planetary non-circular gearing system of the rice transplanters. Xiong Zhao et al. (2020) continued to improve the elliptical gears in this machine and apply them in transplanting machines for other agricultural vegetables [2,3]. In [4], Erika Ottaviano used the elliptical gear-train in the mechanical blood pump for heart surgery. By combining non-circular gears with circular spur gears, Guiyun Xu et al. [5] designed a gearbox for gas discharge machines in the mining industry. JianGang Li et al. [6] utilized a generating gear in the shaping process on the EDM machine for manufacturing non-circular planetary gearing system of the hydraulic motors etc. In the field of designing the elliptical gear train, there are two following main trends: (1) Design of centrode of the gear pair with rotation center located at the foci [4–13] or the center of the ellipse [14–16]; (2) Design of gear profile by (a) Using improve cycloid and cycloid curves as tooth profiles of non-circular gears in the rotor design of Roots-type volumetric hydraulic machines [17–23]; (b) Using generating trapezoidal [12,14] or circular-arc rack cutters [13]; (b) Using generating shaper cutter [24]. When generating by the rack cutter, most of the research focused on the application involute of a circle. For example, the gear profile generated by the rack cutter with an equivalent circle inner [25]; The drawbacks of this method are the narrow addendum of the teeth located close to the major axis. Biing in [16] solved this problem by shifting the rack cutter, which also caused the error of transmission ratios. Therefore, this solution can only apply to non-circular gear pumps. For the elliptical gears, the mating profiles $\{ G_1 \}$, $\{ G_2 \}$ are rolling and sliding with each other at the contact point K. A relative sliding velocity between two profiles on the common tangent *tt'* will cause profile wear from a kinematic aspect. In particular, for the central elliptical gear, the position of the teeth profile $\{\Gamma\}$ of the teeth relative to the center of rotation is not equal. It leads to uneven abrasive on the tooth surface between the teeth on gear during the working process. On the other hand, the pressure angle of the rack cutter determines the geometry of the shaped tooth profile. Therefore, in designing the tooth profile, it is necessary to choose

Cite this article : Thai N H, Thom P V, Lam D B. **Effects of pressure angle on uneven wear of a tooth profile of an elliptical gear generated by ellipse involute** . *Sci. Tech. Dev. J.;* 24(3):2031-2043.

the pressure angle of the rack cutter to avoid this phenomenon.

In this work, the authors applied the elliptical involute in designing gear profile and shifted the elliptical centrode to keep the function of the transmission ratio unchanged. Moreover, when designing the rack cutter, selected different elliptical arcs at other generating ellipse locations to change the pressure angle and avoid causing a narrow addendum. The profile slippage and the number of mating tooth pairs are also considered while selecting the curved segment of the ellipse involute.

DETERMINATION OF THE RELATIVE SLIDING VELOCITY OF THE MATING TOOTH PROFILES

Design parameters of the generating rack cutter for ellipse involute

Given are the centrode of the elliptical gear $\{\Sigma_{EC}\}$, the function of the transmission ratio, and center distance. It is necessary to find the design parameters of the rack cutter for generating the elliptical gear pair with the given function of transmission ratio. Assume that $\{\Sigma_{AE}\}$ is an addendum ellipse, $\{\Sigma_{BE}\}$ is a base ellipse for generating involute arc $\{\Gamma\}$ of the gear; nn' is the pitch line of the rack cutter. During generating process, the line nn' rolls without slipping on $\{\Sigma_{EC}\}$ at the contact points I as described in Figure 1. If tt' is the tangent of $\{\Gamma\}$ at I, then the normal of $\{\Gamma\}$ at I will be a line Δ. Δ will also be the tangent to the base ellipse $\{_{BE}\}$ at the contact point P, and therefore tt' is the profile of the rack cutter. In other words, Δ is the generating line in the form of the elliptical involute $\{\Gamma\}$ and $\alpha_c = \angle(\triangle, nn')$ is the pressure angle of the rack cutter. With each arbitrary point I on$\{\Sigma_{BE}\}$, we can fully generate the elliptical involute arc $\{\Gamma\}$ and corresponding pressure angle αc of the rack cutter. From that, it is possible to determine parameters of $\{\Sigma_{BE}\}$ and$\{\Sigma_{AE}\}$, as well as the other design parameters of the rack cutter as follows.

Parameters of the rack cutter

p_c - the pitch

In the generating process between the gear and the rack cutter, the pitch line nn' rolls without slipping on the centrode $\{\Sigma_{EC}\}$ of the gear. Therefore, the pitch of the rack cutter is equal to the pitch p_c on the centrode $\{\Sigma_{EC}\}$:

$$p_c = \frac{C_{\Sigma_{EC}}}{z} \tag{1}$$

Where: z is the number of teeth, $\Sigma_{z_{EC}}$ is the perimeter of the elliptical centrode $\{\Sigma_{EC}\}$ and is given by the following formula: $C_{\Sigma_{EC}} = \int_0^{2\pi} \sqrt{r_{EC}(\phi)^2 + \left(\frac{dr_{EC}(\phi)}{d\phi}\right)^2} d\phi$, $r_{EC}(\phi)$ is the polar radius of $\{\Sigma_{EC}\}$, and from [19,21], it can be expressed as:

$$r_{EC}(\phi) = \frac{2a_{EC}b_{EC}}{(a_{EC}+b_{EC}) - (a_{EC}-b_{EC})\cos 2\phi} \tag{2}$$

The tooth thickness s and space width w on the pitch line of the rack cutter are expressed by:

$$s = w = \frac{p_c}{2} \tag{3}$$

m_R– module of the rack cutter

$$m_R = \frac{p_c}{\pi} \tag{4}$$

h – the tooth height

The addendum height h_a and the dedendum height h_f are given by:

$$\begin{cases} h_f = k_f m_R \\ h_a = k_a m_R \\ h = (k_a + k_f) m_R \end{cases} \tag{5}$$

With k_f, k_a are the addendum and dedendum height coefficients.

Determination of parameters of the addendum ellipse $\{\Sigma_{AE}\}$ and the base ellipse $\{\Sigma_{BE}\}$ by the design parameters of the rack cutter

From Figure 1a, the parameters of the addendum ellipse $\{\Sigma_{AE}\}$ are:

$$\{\Sigma_{AE}\}: \begin{cases} a_{AE} = a_{EC} + h_a \\ b_{AE} = b_{EC} + h_a \end{cases} \tag{6}$$

And the parameters of the base ellipse are given as below:

$$\{\Sigma_{BE}\}: \begin{cases} a_{BE} = a_{EC} - h_f \\ b_{BE} = b_{EC} - h_f \end{cases} \tag{7}$$

A mathematical model of the profile of the elliptical gear

An equation of the elliptical involute profile

In the fixed coordinate system $\vartheta_f\{O_f, x_f, y_f\}$ in Figure 2a, the generating movement between the gear and the rack cutter consists of: (i) translational movement of the rack in the direction of $O_f x_f$ in distance a_{EC} from O_f; (ii) The gear will: (a) Translate a distance $\triangle s_3(\phi)$ in the direction of $O_f y_f$, (b) Rotate around the gear center O_1 an angle ψ_1. If r_{K_R} is a vector determining position of a point K on profile $\{\Gamma_R\}$ of the gear in the coordinate system $\vartheta_c\{O_c, x_c, y_c\}$ of

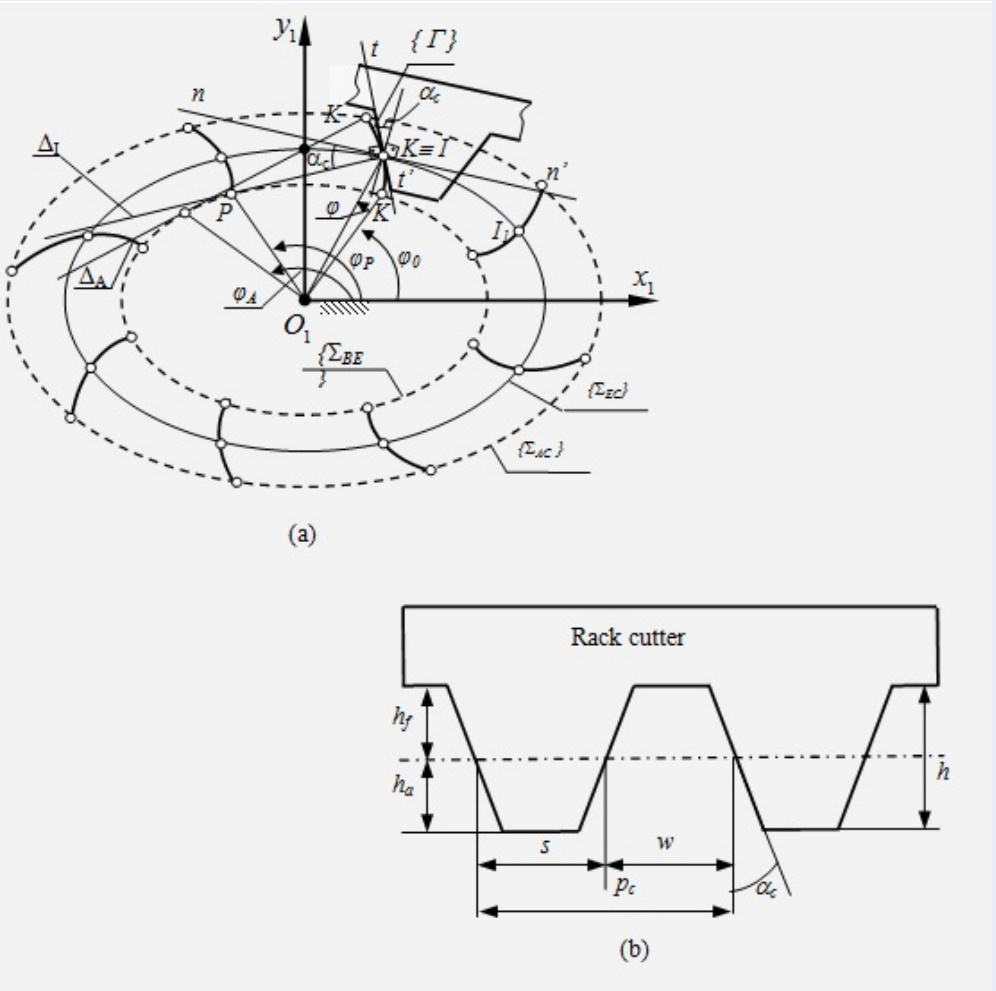

Figure 1: Principle of the shaping elliptical gear with (a) create the shape of the tooth profile with an ellipse involute and (b) Rack cutter

the rack cutter (Figure 2b), and r_{K_E} is a vector determining the position of K on profile $\{\Gamma_E\}$ of the gear in the coordinate system $\vartheta_1\{O_1, x_1, y_1\}$ (see Figure 1a). At the time of generating process $K_\Gamma \equiv K_R \equiv K$, to transfer coordinates of the point K_Γ from coordinate system $\vartheta_c\{O_c, x_c, y_c\}$ to coordinate system $\vartheta_1\{O_1, x_1, y_1\}$ we have the equation of the profile of the elliptical gear as follows:

$$r_{K\Gamma} = {}^1M_f M_f^f M_R^c r_{K_R} \quad (8)$$

Wherein:

$${}^fM_R = \begin{bmatrix} 1 & 0 & s_2 \\ 0 & 1 & -a_{EC} \\ 0 & 0 & 1 \end{bmatrix},$$

$$M_f = \begin{bmatrix} 1 & 0 & 0 \\ 0 & 1 & \triangle s_3(\phi) \\ 0 & 0 & 1 \end{bmatrix},$$

$${}^1M_f = \begin{bmatrix} \cos\psi_1 & \sin\psi_1 & 0 \\ -\sin\psi_1 & \cos\psi_1 & 0 \\ 0 & 0 & 1 \end{bmatrix},$$

With: $s_2(\phi) = s_1(\phi) + r_{EC}(\phi)\cos\mu, \triangle s_3(\phi) = a_{EC} - s_3(\phi) = a_{EC} - r_{EC}(\phi)\sin\mu$

$\psi_1 = \phi + \mu - \frac{\pi}{2}$, $\mu = arc\tan\left(\frac{r_{EC}(\phi)}{dr_{EC}/d(\phi)}\right)$, $r_{EC}(\phi)$ is the polar radius of $\{\Sigma_{EC}\}$, ϕ is the angle determining the arc $\overset{J}{e}$ of $\{\Sigma_{EC}\}$ when $\{\Sigma_{EC}\}$ rolls without slipping on the rack cutter datum line from

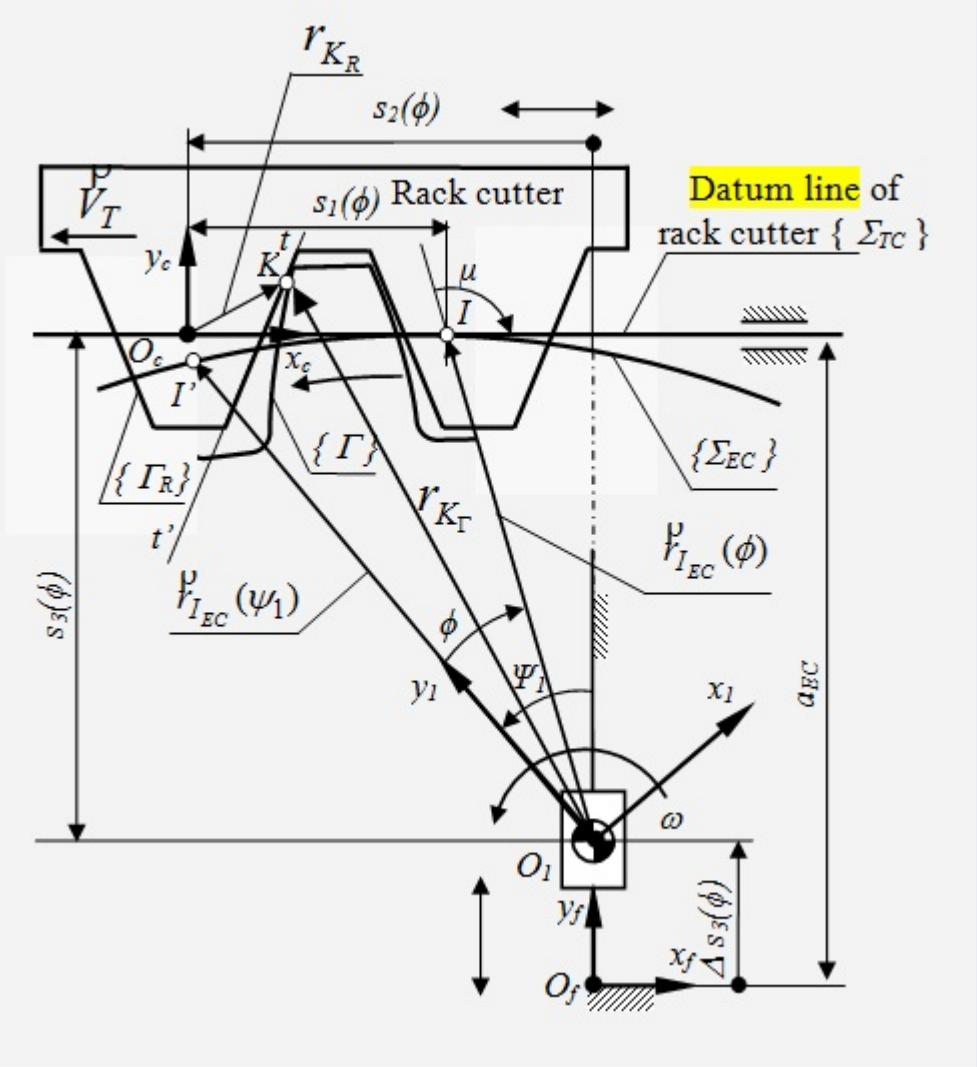

Figure 2: Relative movement between the rack cutter and elliptical gear during machining

the position I to position I'. At the same time, the rack cutter will translate a distance $s_1(\phi) = \overset{J}{e} = \int_0^\phi \left((r_{EC}(\phi))^2 + \left(\frac{dr_{EC}(\phi)}{d\phi} \right)^2 \right)^{0.5} d\phi$. The parameters $l_i(\phi)$, $\theta_i(\phi)$ in Figure 2b are taken from gearing condition between the rack cutter and the gear at K.

Undercutting

Litvin in [12,25] stated that for avoiding undercutting phenomenon, a module m_R of the rack cutter must satisfy the following condition:

$$\begin{vmatrix} \frac{dx_{K_R}}{dl} & -{}^c v_{trx} \\ \frac{\partial f(\phi)}{\partial \lambda} & \frac{\partial f(\phi)}{\partial \phi}\frac{d\phi}{dt} \end{vmatrix} = \begin{vmatrix} \frac{dy_{K_R}}{dl} & -{}^c v_{try} \\ \frac{\partial f(\phi)}{\partial \lambda} & \frac{\partial f(\phi)}{\partial \phi}\frac{d\phi}{dt} \end{vmatrix} \neq 0 \quad (9)$$

Where: $f(\phi)$ is determined from gearing condition between the rack cutter and the gear, ${}^c v_{trx}$, ${}^c v_{try}$ are components of the relative sliding velocity of K on $\{\Gamma_R\}$ of the rack cutter. Condition for avoiding undercutting is obtained by solving equation (9):

$$m_R \leq \rho_{min} \sin^2 \alpha_c \quad (10)$$

With ρ_{min} is the minimum curvature radius of $\{\Sigma_{EC}\}$:

$$\rho_{min} = \frac{a_{EC} b_{EC}}{2a_{EC} - b_{EC}} \quad (11)$$

ESTABLISHMENT OF THE SLIPPAGE COEFFICIENTS

Equation of the sliding velocity at the meshing point

In the fixed coordinate system $\vartheta_f\{O_f, x_f, y_f\}$ attached to the rotation center of the gear 1, with conjugated profiles ($\{\Gamma_1\}$, $\{\Gamma_2\}$) where $\{\Gamma_1\}$ and $\{\Gamma_2\}$ belong to the first and second gear, respectively. At the moment of meshing on the arbitrary point K, the common normal nn' of $\{\Gamma_1\}$ and $\{\Gamma_2\}$ intersect $\overline{O_1O_2}$ at I *(I is the pitch point of the gear pair).*

In Figure 3, ρ_{K_1}, ρ_{K_2} are meshing radii from point K to the centers O_1, O_2. When the gear 1 rotates clockwise with angular velocity ω_1, the gear 2 will rotate with $\omega_2 = \frac{\omega_1}{i_{12}(\psi_1)}$, where $i_{12}(\psi_1)$ is the gear ration function. The absolute velocities of $K_1 \in \{\Gamma_1\}$, $K_2 \in \{\Gamma_2\}$ in the $\vartheta_f\{O_f, x_f, y_f\}$ are given by:

$$\begin{cases} V_{K_1} = \rho_1(\psi_1)\,\omega_1 \\ V_{K_2} = \rho_2(\psi_2(\psi_1))\,\omega_1\,(i_{12}(\psi_1))^{-1} \end{cases} \quad (12)$$

Where: $\rho_1(\psi_1) = \sqrt{[r_{K_1}(\psi_1)]^T [r_{K_1}(\psi_1)]}$

$\rho_2(\psi_2(\psi_1)) = \sqrt{[r_{K_1}(\psi_1) - r_{O_2}]^T [r_{K_1}(\psi_1) - r_{O_2}]}$

With $r_{O_2} = [A_{12} \quad 0]^T$

If $V^t_{K_1}$, $V^t_{K_2}$ are tangential components of $V^\mu_{K_1}$, $V^\mu_{K_2}$ projected to the common tangent tt', we will have following equations:

$$\begin{cases} V^t_{K_1} = V_{K_1}\cos\beta_1(\psi_1) \\ V^t_{K_2} = V_{K_2}\cos\beta_2(\psi_2(\psi_1)) \end{cases} \quad (13)$$

Where: $\beta_1(\psi_1) = \angle\left(\overrightarrow{V}_{K_1}, tt'\right)$, $\beta_2(\psi_2(\psi_1)) = \angle\left(\overrightarrow{V}_{K_2}, tt'\right)$ are expressed by:

$$\begin{cases} \beta_1(\psi_1) = \frac{\pi}{2} - arc\cos\left(\frac{\overrightarrow{n}_K(\psi_1)\overrightarrow{V}_{K_1}(\psi_1)}{||\overrightarrow{n}_K(\psi_1)||\left|\left|\overrightarrow{V}_{K_1}(\psi_1)\right|\right|}\right) \\ \beta_1(\psi_2(\psi_1)) = \frac{\pi}{2} - arc\cos\left(\frac{\overrightarrow{n}_K(\psi_2)\overrightarrow{V}_{K_2}(\psi_2(\psi_1))}{||\overrightarrow{n}_K(\psi_2)||\left|\left|\overrightarrow{V}_{K_2}(\psi_2(\psi_1))\right|\right|}\right) \end{cases} \quad (14)$$

In (14), we have: $n_K = [(x_K(\psi_1) - \rho_I) \quad y_K(\psi_1)]^T$

Finally, the velocity of relative slippage between $K_1 \in \{\Gamma_1\}$ and $K_2 \in \{\Gamma_2\}$ is calculated as follows:

$$\begin{cases} V^{tr}_{K_{12}} = V^{tr}_{K_1}(\psi_1) - V^{tr}_{K_2}(\psi_2(\psi_1)) \\ V^{tr}_{K_{21}} = V^{tr}_{K_2}(\psi_2(\psi_1)) - V^{tr}_{K_2}((\psi_1)) \end{cases} \quad (15)$$

Establishing the equation of the profile coefficients

When the centered elliptical gears are meshing, the point K moves along the line of action, and if K is not at the same position as I is, then profile slippage occurs. To examine the influence of the slippage on the profile wear, the slippage coefficient μ is proposed [19,26]:

$$\begin{cases} \mu_1(\psi_1) = \frac{V^{tr}_{K_{12}}(\psi_1)}{V^{tr}_{K_1}(\psi_1)} \\ \mu_2(\psi_2(\psi_1)) = \frac{V^{tr}_{K_{21}}(\psi_2(\psi_1))}{V^{tr}_{K_2}(\psi_2(\psi_1))} \end{cases} \quad (16)$$

By substituting (15) into (16), we have:

$$\begin{cases} \mu_1(\psi_1) = 1 - \frac{V^{tr}_{K_2}(\psi_2(\psi_1))}{V^{tr}_{K_1}(\psi_1)} \\ \mu_2(\psi_2(\psi_1)) = \frac{V^{tr}_{K_1}(\psi_1)}{V^{tr}_{K_2}(\psi_2(\psi_1))} \end{cases} \quad (17)$$

INFLUENCE OF THE PRESSURE ANGLE OF THE RACK CUTTER ON THE PROFILE SLIPPAGE

A software program evaluating the influence of the rack cutter pressure angle on the profile slippage has developed from the established mathematical model. The authors present case study of the elliptical gear train with the centrode $\{\Sigma_{EC}\}$: major- semi axis $a_{EC} =$ 40 mm, minor-semi axis $b_{EC} = 24$ mm and axis distance $A_{12} = 64$ mm. To examine the influence of the pressure angle on the slippage coefficients curve, the addendum and dedendum coefficient were selected $k_a = 1.15$, $k_f = 1.35$, respectively, to avoid teeth interference. By substituting to equations (6, 7), we have the parameters of the addendum ellipse $\{\Sigma_{AE}\}$: $a_{AE} =$ 42.1055 mm, $b_{AE} = 26.1055$ mm, and those of the base ellipse $\{\Sigma_{BE}\}$: $a_{BE} = 37.5283$ mm, $b_{BE} = 21.5283$ mm. And after substituting the parameters of the centrode $\{\Sigma_{EC}\}$: a_{EC}, b_{EC} to (11), we obtain $\rho_{min} = 17.14$ mm. To avoid undercutting, after choosing $\rho_{min} =$ 17.14 mm in (10), we have $m_{max} = 1.8309$. Combining with $m = 1.8$ mm, by substitution to (4), the number of teeth is z = 36. Because of the symmetry of the elliptical semiaxes, the involute arcs of the base ellipse in the first quarter presented in Figure 4.

From Figure 4, the pressure angles α_c of the rack cutter corresponding to the elliptical involute arcs at different locations I_i (the pitch point) on $\{_{EC}\}$ shown in Table 1. Only four points I_1, I_2, I_3, I_4satisfy a condition for avoiding interference and undercutting.

With obtained data, we present the results for 4 cases at the position when the meshing process begins with the pair of profiles ($\{\Gamma_1\}$, $\{\Gamma_2\}$) of the tooth number 1 of the first gear and the tooth number 19 of the second gear. At the meshing position shown in Figure 4b, the angular velocity w of the driving gear 1 selected to be equal to 15 rad/s:

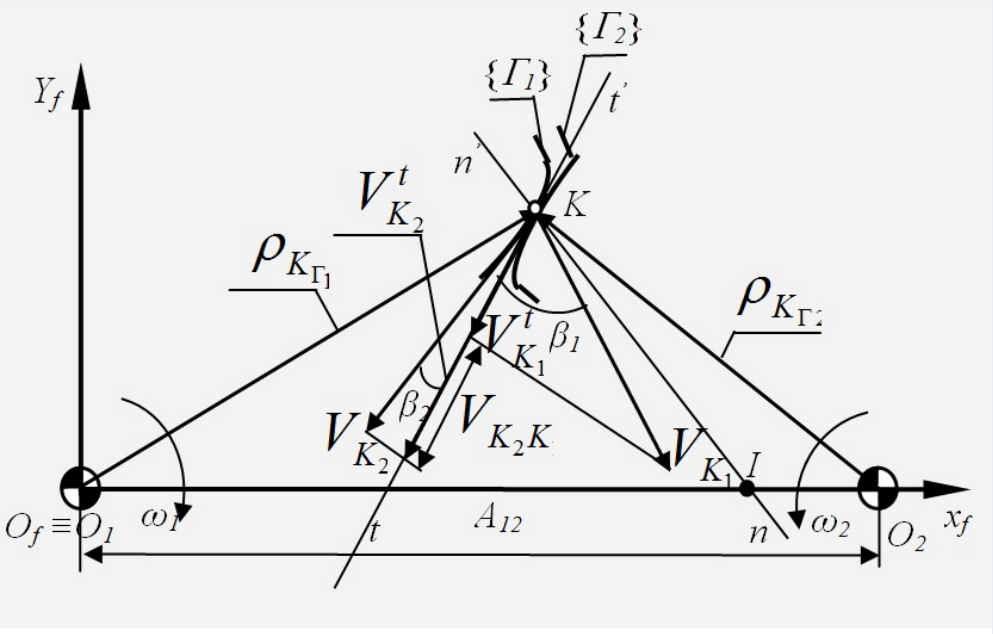

Figure 3: Kinematic relation at the contact point between two profiles reciprocal

Table 1: Pressure angles corresponding to elliptical involute arcs at *I* on $\{\Sigma_{EC}\}$

Position	I_0	I_1	I_2	I_3
α_c [^{o}]	30.5	28	25	22.5
Position	I4	I5	I6	I7
α_c [^{o}]	20	18.2	15.5	13

Case 1: *The elliptical involute arc is at the position* $I_4(\alpha_c = 20^o)$

From Figure 5a, it is noticeable that with the given direction of rotation in Figure 4b, tooth number 1 of the first gear begins to mesh with tooth number 19 of the second gear. During the meshing process, the contact point K will move along the profile $\{\Gamma_1\}$ from the starting position to the addendum. At the same time, along with the conjugated profile $\{\Gamma_2\}$ the point K moves from the addendum to the dedendum area. Figure 5b shows the graph describing a relation between the slippage coefficients μ_1, μ_2. At pitch point I, there is no slippage between the profiles, which means that only rolling movement happens. Moreover, in this case, the dedendum of the first gear is less worn than the second gear, but the addendum of the second gear is worn more than the first gear.

Case 2: *The elliptical involute arc is at the position* I_3 $(\alpha_c = 22.5^o)$

In this case, the addendum of the first gear becomes narrower, the size of the dedendum increases, and absolute values of the slippage coefficients μ_1, μ_2 are 0.05 larger than those in the previous case (Figure 5b and Figure 6b).

Case 3: *The elliptical involute arc is at the position* I_2 $(\alpha_c\alpha_c\alpha_c = 25^o)$

Figure 7a shows tooth number 19 of the second gear at the position of the maximum curvature radius. The tooth profile turns into a straight one, similarly to the profile of the rack. And tooth number 1 of the first gear is at the position of the minor-semi axis, where the tooth has a larger dedendum and narrower addendum. In this case, the conjugated profiles will be evenly worn, but the dedendum of tooth number 1 of the first gear (position at the minor-semi axis) will be worn faster.

Case 4: *The elliptical involute arc is at the position* I_2 $(\alpha_c\alpha_c\alpha_c\alpha_c\alpha_c = 2$

In Figure 8a, we can notice that the space width will be narrowest at tooth number 19 of the second gear (position at the minor-semi axis). The slippage coefficients increase at the dedendum of the first gear,

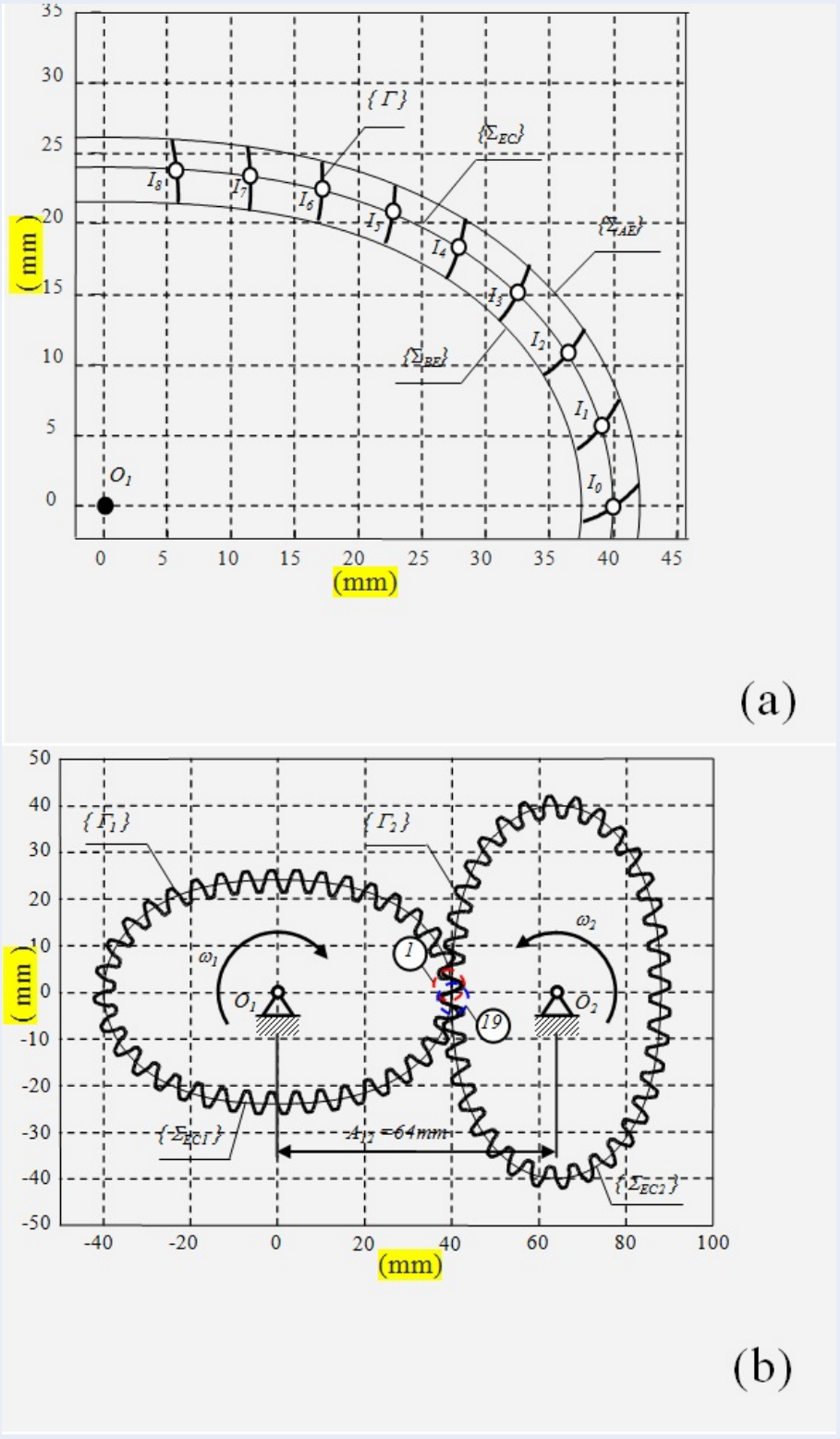

Figure 4: The elliptical involute gear with (a) elliptical involute arcs of the base ellipse Σ_{EC} (b) the elliptical gear with involute profile at I_4

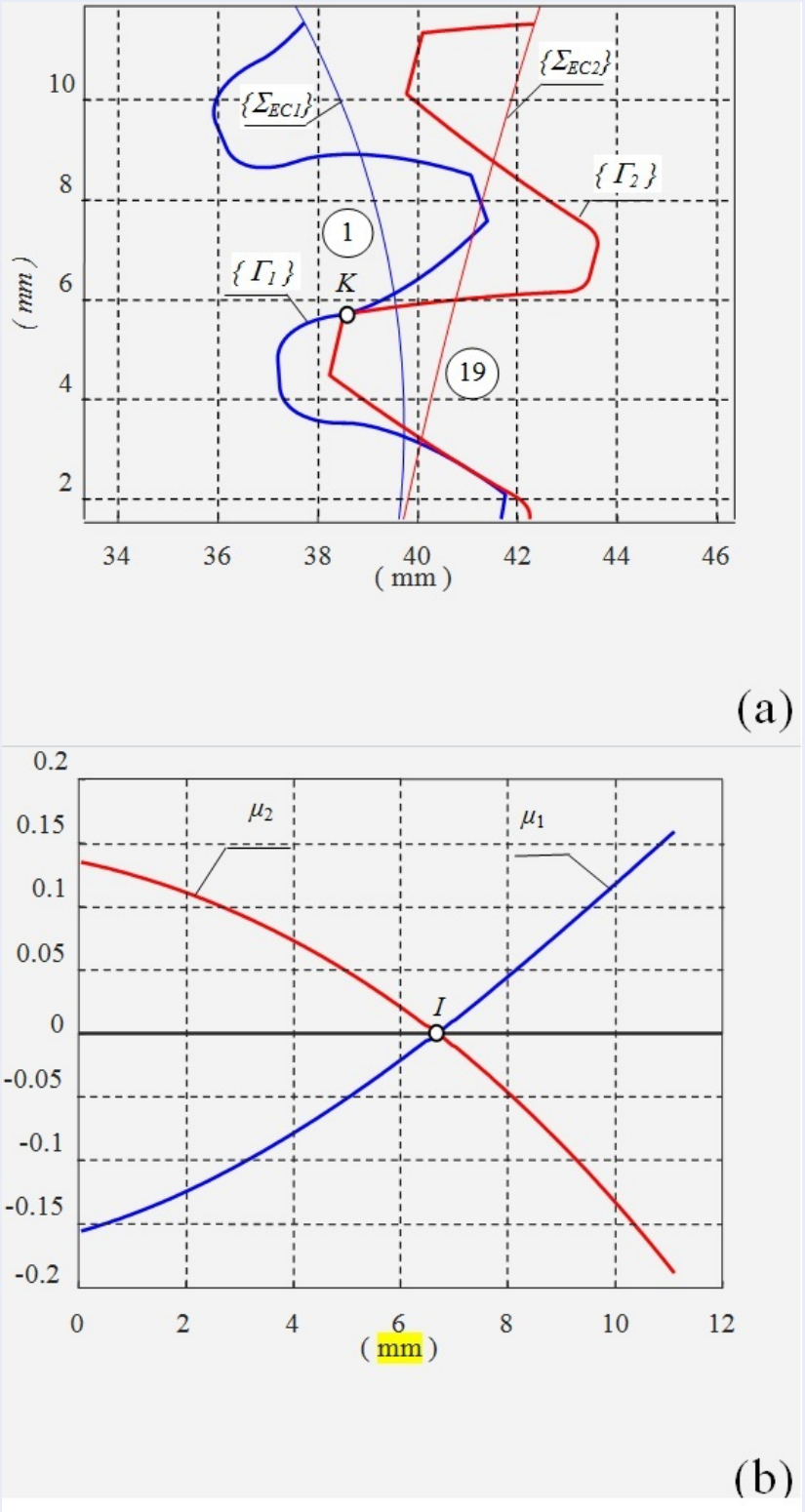

Figure 5: The conjugated profiles generated by the rack with the pressure angle $\alpha_c = 20^o$ with (a) conjugated profiles at the beginning of the meshing process and (b) graph of slippage coefficients.

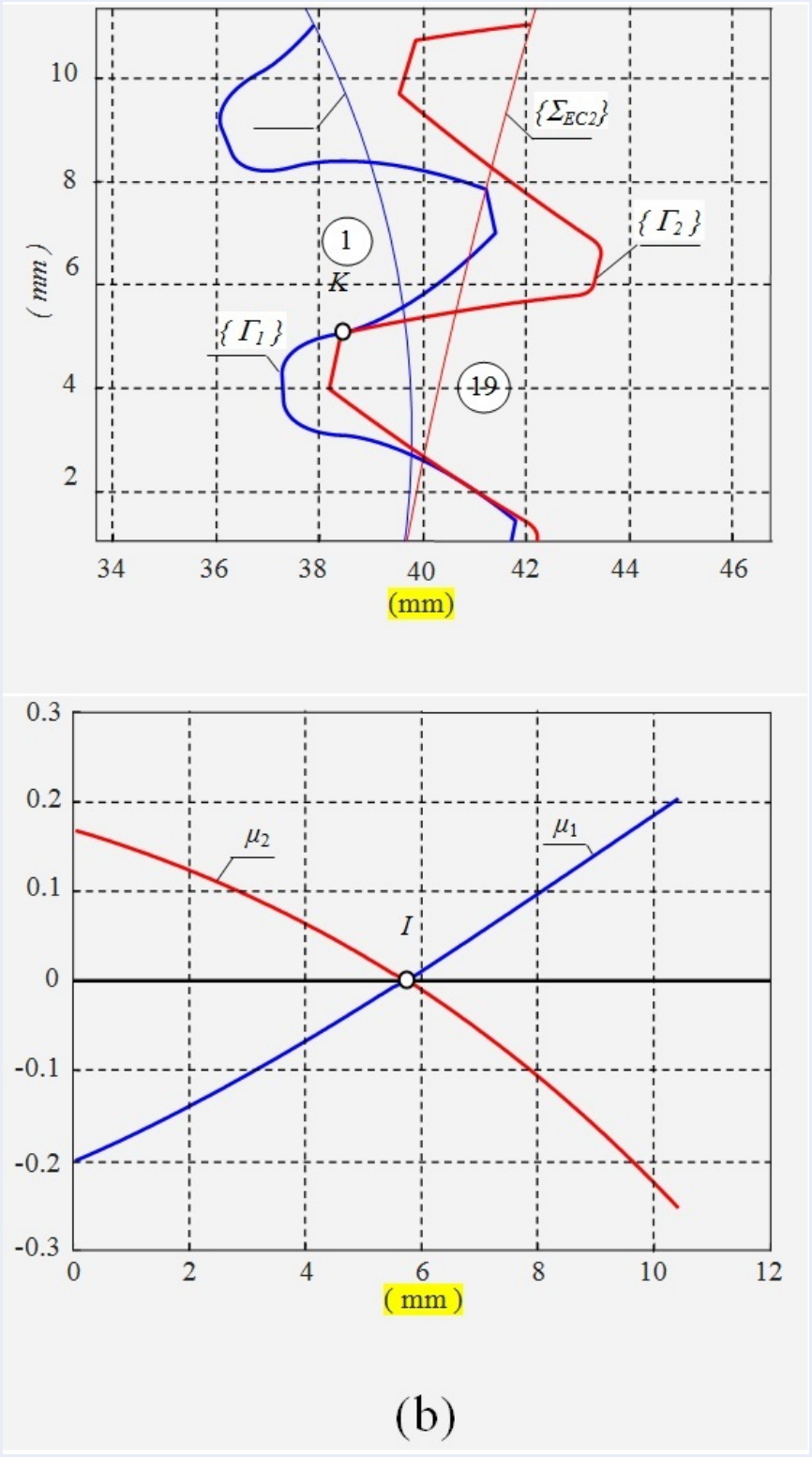

Figure 6: The conjugated profiles generated by the rack with the pressure angle $\alpha_c = 22.5$: (a) conjugated profiles at the beginning of meshing process and (b) graph of slippage coefficients

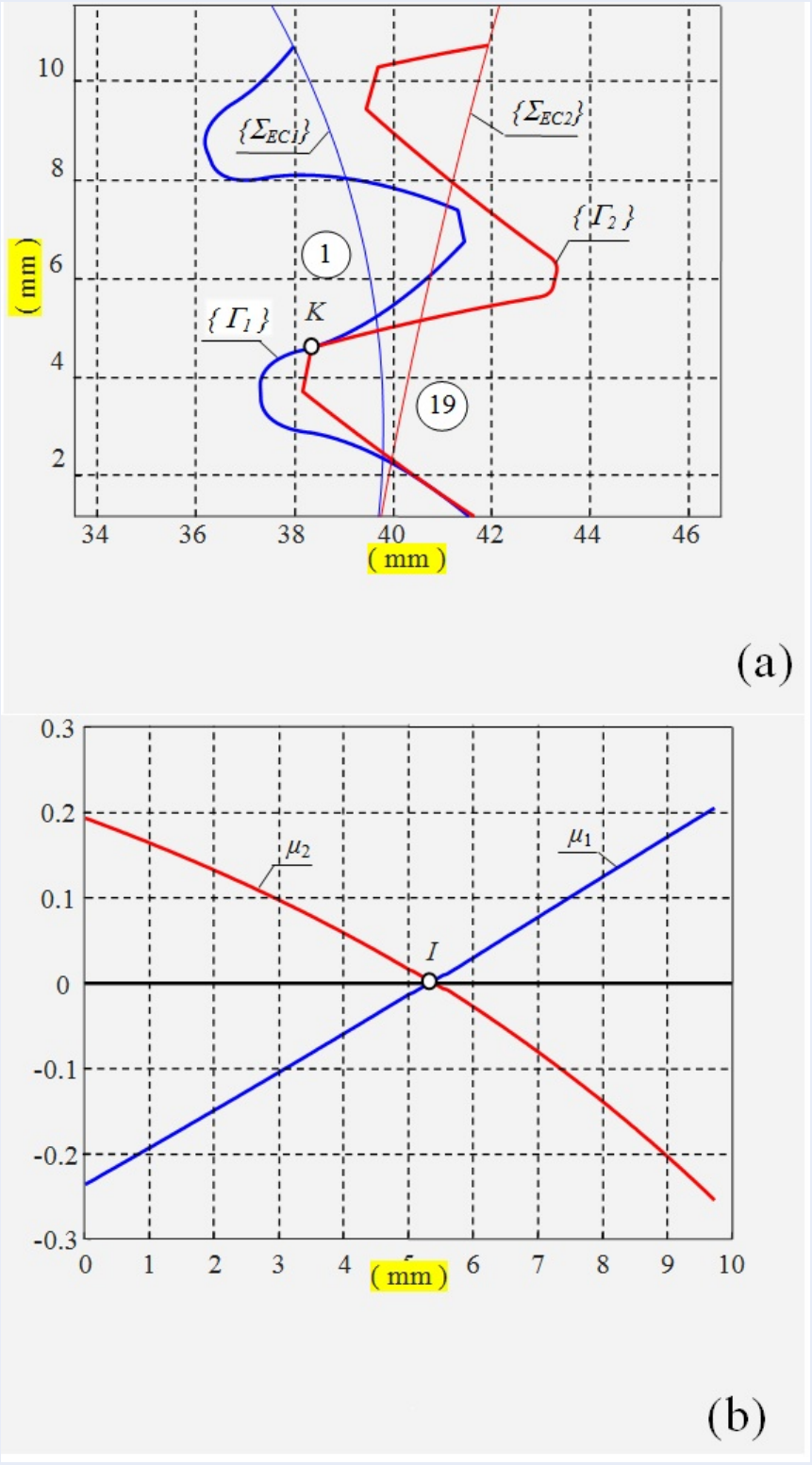

Figure 7: The conjugated profiles generated by the rack with the pressure angle $\alpha_c.\alpha_c.\alpha_c.\alpha_c.\alpha_c.\alpha_c = 25$: (a) conjugated profiles at the beginning of meshing process and (b) graph of slippage coefficients.

which means rising pressure angle causes enlargement of the slippage coefficient and leads to faster wearing of the teeth.

DISCUSS THE RESULTS

From the above numerical calculation results, we can notice the following points:

(1) As the pressure angle value of the rack cutter increases, then the working arc length on the tooth profile decreases. If L is called the length of the meshing arc on the tooth profile (from point meshing into to point meshing out), then: $L|_{\alpha_c} = 20^\circ$ mm, $L|_{\alpha_c} = 22.5^\circ$ mm, $L|_{\alpha_c} = 25^\circ$ mm, $L|_{\alpha_c} = 28^\circ$ mm. While the length meshing arc on root teeth (from point meshing into to pitch point) increases, the length meshing arc on top teeth (from the pitch point to point meshing out) decreases (see Figure 9).

(2)To achieve thorough evaluation, we use $\triangle\mu = |\mu_1 - \mu_2|$ to demonstrate the difference between slippage coefficients during the meshing process (Figure 9). We have:

(i) When the pressure angle a_c of the rack cutter increases, the elliptical gear with an involute profile will have the teeth in the area close to the minor-semi axis with the narrower addendum. And the teeth close to the major-semi axis will have a narrower dedendum, which leads to a meshing zone between conjugated teeth.

(i) When $\triangle\mu$ (difference between slippage coefficients of dedendum and addendum, respectively) increases, which means the pressure angle of the rack cutter will have larger values, the gear will be worn faster, especially with the teeth located close to minor-semi axes and major-semi axes. However, the distance from the starting point of the mesh cycle to the pitch point will be shorter, enhancing the teeth' bending resistance and making those gears suitable for the high-load application.

CONCLUSIONS

The findings of this work were as follows:

(i) Research has built a mathematical model for evaluating and selecting the elliptical involute arc on the centrode and the rack cutter's pressure angle α_C to reduce profile slippage and uneven wear of the elliptical gears pair.

(ii) Successfully developed the software program to examine and select appropriate involute arc of the base ellipse for gear profile design.

(iii) It confirmed that with higher values of the rack pressure angle, the profile wear would happen faster because of the higher differences between slippage coefficients of the tooth addendum and dedendum, respectively. Moreover, the addendum of the teeth close to the minor-semi axis will narrower, and the dedendum of the teeth close to the major-semi axis will also have a smaller width.

CONFLICT OF INTERESTS

The authors declared no potential conflicts of interest with respect to the research, authorship, and publication of this article.

AUTHOR CONTRIBUTION

The initiative idea, theoretical modeling, implementation plan, and write of the paper were made by the author Nguyen Hong Thai; The author Phung Van Thom programmatically and simulates; Author Dang Bao Lam contributes ideas and corrects the paper. The manuscript was written through the contribution of all authors. All authors discussed the results, reviewed and approved the final version of the manuscript.

REFERENCES

1. Guo LS, Zhang WJ. Kinematic analysis of a rice transplanting mechanism with eccentric planetary gear trains. Mechanism and Machine Theory. 2001;(36):1175 - 1188;Available from: https://doi.org/10.1016/S0094-114X(01)00052-0.
2. Zhao X, et al. Research on design method of non-circular planetary gear train transplanting mechanism based on precise poses and trajectory optimization. Advances in Mechanical Engineering. 2018;10(12):1-12;Available from: https://doi.org/10.1177/1687814018814368.
3. Zhao X, et al. Automatic Scallion Seedling Feeding Mechanism with an Asymmetrical High-order Transmission Gear Train. Chinese Journal of Mechanical Engineering. 2020;33(1):2-14;Available from: https://doi.org/10.1186/s10033-020-0432-9.
4. Ottaviano E, et al. Numerical and experimental analysis of non-circular gears and cam-follower systems as function generators. Mechanism and Machine Theory. 2008;(43):996-1008;Available from: https://doi.org/10.1016/j.mechmachtheory.2007.07.004.
5. Xu G, et al. Design and Performance Analysis of a Coal Bed Gas Drainage Machine Based on Incomplete Non-Circular Gears. Energies. 2017;p.2-19;Available from: https://doi.org/10.3390/en10121933.
6. Li J, et al. Numerical computing method of non-circular gear tooth profiles generated by shaper cutters. Int J Adv Manuf Technol. 2007;(33):1098-1105;Available from: https://doi.org/10.1007/s00170-006-0560-0.
7. Tsay MF, Fong ZH. Study on the Generalized Mathematical Model of Non-circular Gears. Mathematical and Computer Modelling. 2005;(41):555-569;Available from: https://doi.org/10.1016/j.mcm.2003.08.010.
8. Figliolini G, Angeles J. The Synthesis of Elliptical Gears Generated by Shaper-Cutters, Journal of Mechanical Design. 2003;(125): 793- 801;Available from: https://doi.org/10.1115/1.1631573.
9. Xia L, Liu Y, Li D, Han J. A linkage model and applications of hobbing non-circular helical gears with axial shift of hob, Mechanism and Machine Theory. 2013;(70):32-44;Available from: https://doi.org/10.1016/j.mechmachtheory.2013.07.002.
10. Karpov O, Nosko P, et al. Prevention of resonance oscillations in gear mechanisms using non-circulargears, Mechanism and Machine Theory. 2017; (114):1-10;Available from: https://doi.org/10.1016/j.mechmachtheory.2017.03.010.

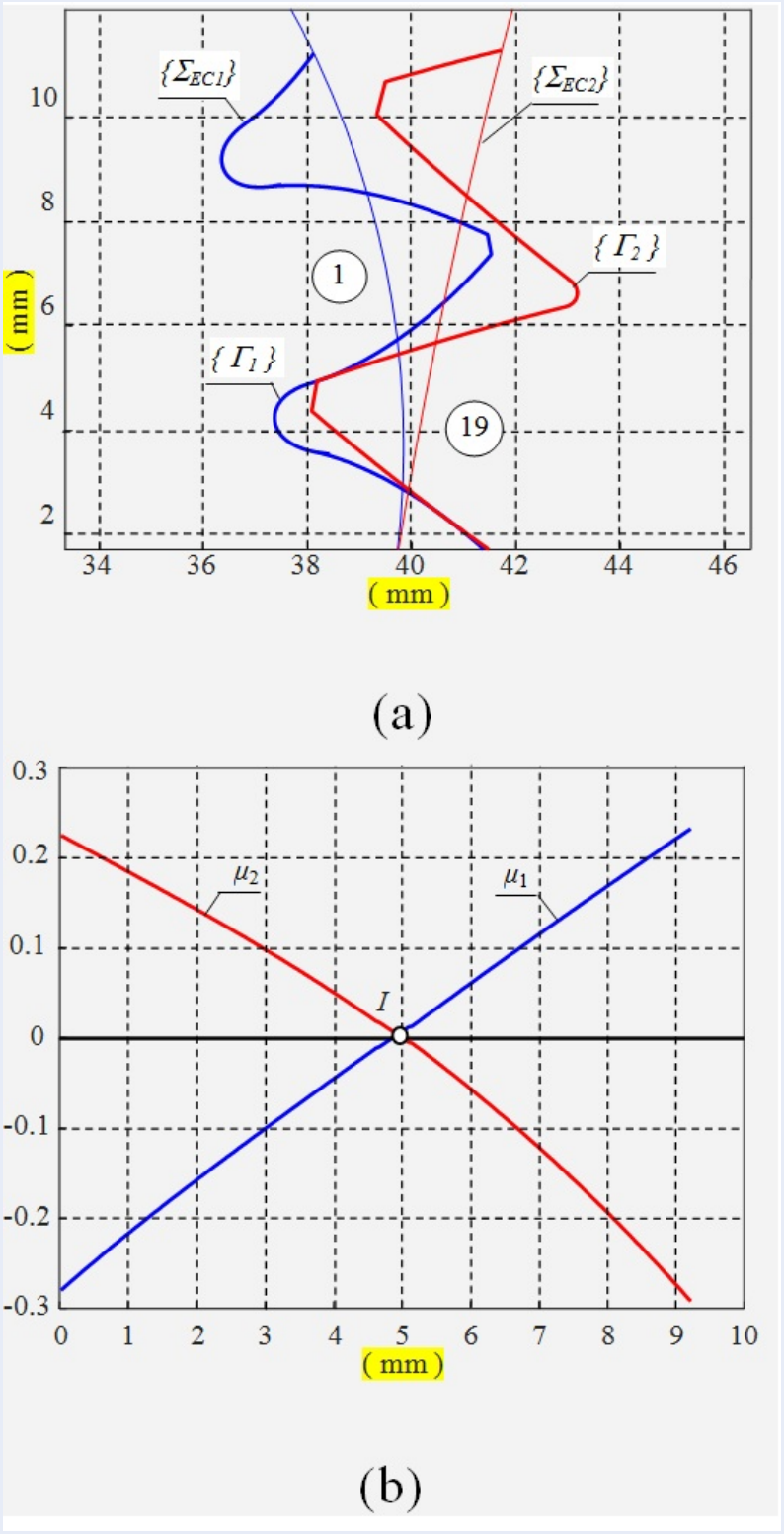

Figure 8: The conjungated profiles generated by the rack with the pressure angle $\alpha_c = 28$: (a) conjungated profiles at the beginning of meshing process and (b) graph of slippage coefficients.

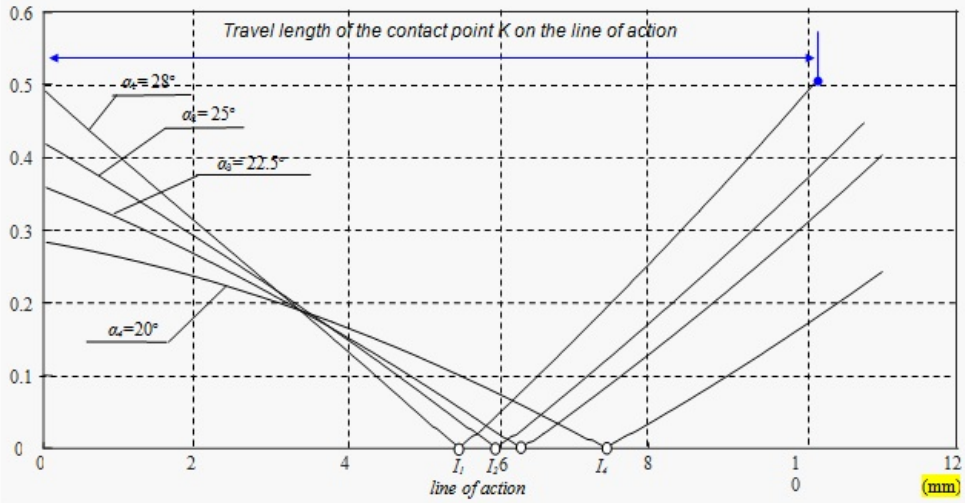

Figure 9: Values of $\triangle\mu$ corresponding to different pressure angles of the rack cutter.

11. Riaza HFQ, Foix SC, Nebot LJ. The Synthesis of anN-Lobe Non-circular Gear Using Bézier and B-Spline Nonparametric Curves in the Design of Its Displacement Law, Journal of Mechanical Design. 2007;(129): 981-985;Available from: https://doi.org/10.1115/1.2780771.
12. Litvin FL, Gonzalez-Perez I, et al. Generation of planar and helical elliptical gears by application of rack-cutter, hob, and shaper. Comput. Methods Appl. Mech. Engrg. 2007;(196):4321-4336;Available from: https://doi.org/10.1016/j.cma.2007.05.003.
13. Chen CF, Tsay CB. Computerized tooth profile generation and analysis of characteristics of elliptical gears with circular-arc teeth. Journal of Materials Processing Technology. 2004;(148):226-234;Available from: https://doi.org/10.1016/j.jmatprotec.2003.07.011.
14. Bair BW, Sung MH, Wang JS, Chen CF. Tooth profile generation and analysis of oval gears with circular-arc teeth. Mechanism and Machine Theory. 2009;(44):1306-1317;Available from: https://doi.org/10.1016/j.mechmachtheory.2008.07.003.
15. Liu X, Nagamura K, Ikejo K. Analysis of the Dynamic Characteristics of Elliptical Gears. Journal of Advanced Mechanical Design, Systems, and Manufacturing. 2012; 6 (4):484-497;Available from: https://doi.org/10.1299/jamdsm.6.484.
16. Bair BW. Computer aided design of non-standard elliptical gear drives. Proc Instn Mech Engrs Vol 216 Part C: J Mechanical Engineering Science. 2001; p 473-483;Available from: https://doi.org/10.1243/0954406021525250.
17. Thai NH, Trung NT. Establishing formulas for design of Roots pump geometrical parameters with given specific flow rate. Vietnam Journal of Science and Technology, Vietnam Academy of Science and Technology. 2015;53(4):533-542;Available from: https://doi.org/10.15625/0866-708X/53/4/3908.
18. Thai NH, Tien TN, Dung PT, Huy NQ. Influence of the Designing Parameters on Flow Fluctuation and Pressure of the Improved Roots Blower, International Conference of Fluid Machinery and Automation Systems - ICFMAS2018. 2018; p. 196-203;.
19. NH Thai, TN Tien. Influence of the designing parameters on the profile slippage and flow of the Roots blower. Science & Technology Development Journal-Engineering and Technology.2018;1(1) p13-9;.
20. Tien TN, Thai NH, Long ND. Effects of head gaps and rotor gap on flow rate and hydraulic leakage of a novel non-contact rotor blower. Vietnam Journal of Science and Technology. (2019), 57(6A):125-125;Available from: https://doi.org/10.15625/2525-2518/57/6A/14466.
21. Tien TN, Thai NH. A novel design of the Roots blower. Vietnam Journal of Science and Technology.(2019);57(2):249-260;Available from: https://doi.org/10.15625/2525-2518/57/2/13094.
22. Thai NH, Long ND. A new design of the Lobe pump is based on the meshing principle of elliptical gear pairs. Science & Technology Development Journal-Engineering and Technology. (2021);4(2):861-871;Available from: https://doi.org/10.32508/stdjet.v4i2.769.
23. Thai NH, Trung NT, Viet NH. Research and manufacture of external non-circular gear-pair with improved cycloid profile of the ellipse. Science & Technology Development Journal-Engineering and Technology.(2021);4(2):835-845;Available from: https://doi.org/10.32508/stdjet.v4i2.773.
24. Zheng F, Hua L, et al. Linkage model and manufacturing process of shaping non-circular gears, Mechanism and Machine Theory. 2016; (96):192-212;Available from: https://doi.org/10.1016/j.mechmachtheory.2015.09.010.
25. Litvin FL. Alfonso Fuentes-Azna, Ignacio Gonzalez-Perez, Kenichi Hayasaka. Noncircular Gears Design and Generation. Cambridge University Press. 2009;Available from: https://doi.org/10.1017/CBO9780511605512.
26. Thai NH, Giang TC. The influence off design parameters on the profile sliding in an internal hypocycloid gear pair. Vietnam Journal of Sience and Technology. 2018;56 (4): 482 - 491;Available from: https://doi.org/10.15625/2525-2518/56/4/9625.